JOURNAL OF VIROLOGY, Nov. 1980, p. 325-336
0022-538X/80/11-0325/12$02.00/0

Vol. 36, No. 2

Identification of the Avian Myeloblastosis Virus Genome

II. Restriction Endonuclease Analysis of DNA from λ Proviral Recombinants and Leukemic Myeloblast Clones

L. M. SOUZA, M. J. BRISKIN, R. L. HILLYARD, AND M. A. BALUDA*

UCLA School of Medicine and Molecular Biology Institute, Los Angeles, California 90024

Two λ proviral DNA recombinants were characterized with a number of restriction endonucleases. One recombinant contained a complete presumptive avian myeloblastosis virus (AMV) provirus flanked by cellular sequences on either side, and the second recombinant contained 85% of a myeloblastosis-associated virus type 1 (MAV-1)-like provirus with cellular sequences adjacent to the 5′ end of the provirus. Comparing the restriction maps for the proviral DNAs contained in each λ hybrid showed that the putative AMV and MAV-1-like genomes shared identical enzyme sites for 3.6 megadaltons beginning at the 5′ termini of the proviruses with respect to viral RNA. Two enzyme sites near the 3′ end of the MAV-1-like provirus were not present in the putative AMV genome. We also examined a number of leukemic myeloblast clones for proviral content and cell-provirus integration sites. The presumptive AMV provirus was present in all the leukemic myeloblast clones regardless of the endogenous proviral content of the target cells or the AMV pseudotype used for conversion. Multiple cellular sites were suitable for integration of the putative AMV genome and the helper genomes. The proviral genomes were all integrated colinearly with respect to linear viral DNA.

A library of λ chicken recombinant phage had been constructed with DNA from avian myeloblastosis virus subgroup B (AMV-B)-producing leukemic myeloblasts (17) to isolate AMV and myeloblastosis-associated virus (MAV) proviruses. One recombinant, λ11A1-1, has been partially characterized with *Eco*RI and *Hin*dIII and shown to contain a complete presumptive AMV provirus flanked on both sides by cellular DNA (17). A second recombinant, λ10A2-1, is characterized herein and contains 85% of a MAV-1-like provirus. In this study we have compared the viral and cellular sequences in λ11A1-1 with those in λ10A2-1 by restriction endonuclease analyses.

Leukemic myeloblasts from the peripheral blood of leukemic chicks contain the putative AMV genome and in most cases a helper genome (16). Juncture fragments are generally not detectable in the leukemic myeloblasts isolated from leukemic chickens (16). Leukemic myeloblast clones were isolated, and their DNA was analyzed by restriction endonuclease digestion and Southern blotting to demonstrate the following: (i) all leukemic myeloblasts contain the putative AMV genome, (ii) helper virus may or may not be present in a leukemic myeloblast, and (iii) integration of the putative AMV genome and the helper genomes can occur at multiple cellular sites.

MAV-1 and MAV-2 and AMV viral DNAs can be distinguished from one another by *Hin*dIII cleavage (3). *Hin*dIII cleaves linear viral DNA of MAV-1 and MAV-2 within 0.2 megadaltons (Md) of both termini and twice more internally in MAV-1 and once internally in MAV-2. The putative AMV provirus is also cleaved within 0.2 Md of both termini as well as at one other internal site (17). *Hin*dIII digestion of chicken embryo fibroblast DNA containing integrated MAV-1 or MAV-2 indicates the DNA intermediates integrate colinearly with respect to their linear viral DNA and outside the two terminal *Hin*dIII sites (3). Therefore, by digesting the leukemic myeloblast clone DNAs with *Hin*dIII, we can identify their proviral content. After inspecting the restriction maps generated for the proviruses in the λ recombinants, we chose *Eco*RI and *Kpn*I for detecting juncture fragments in the leukemic myeloblast clones.

The number of endogenous proviruses and integration sites for these proviruses varies greatly from one chicken strain to another and even within a strain (1, 7, 10, 15). Integration of avian sarcoma virus (ASV) DNA in clones of rat, duck, and quail cells has been characterized (4, 8, 12), but the integration of these exogenous viruses in chicken cells is less well documented. Studies with various clones of ASV-transformed cells indicate that there are many sites for inte-

gration within the cellular DNA, as well as a specific region in the viral DNA for integration (4, 8, 12).

We have found that the putative AMV genome and the genomes of its helper viruses can integrate at multiple sites in the cellular DNA. All of these viruses also integrate colinearly with respect to linear viral DNA at a site(s) on the viral DNA at or very near the termini defined by linear viral DNA.

MATERIALS AND METHODS

Chicken strains and viruses. In addition to the chicken strains used in the accompanying paper (16), the following two strains were used: C/O H&N gs^- chf^- V^- from H&N Farms, Redmond, Wash., and $L7_2$ C/ABE V^+ from the Regional Poultry Laboratory, East Lansing, Mich. The virus stocks used are described in the accompanying paper (16).

Isolation of leukemic myeloblast clones. Yolk sac cultures were prepared from 13-day-old chicken embryos as previously described (2). The embryos were immediately frozen in liquid nitrogen for subsequent DNA extraction to determine the endogenous proviral content. The yolk sac cells were cultured in BM II (2) supplemented with 5% calf serum, 5% heat-inactivated chicken serum, and 10% tryptose phosphate. Yolk sac cells were seeded at approximately 10^6 cells/60-mm dish and infected with AMV-S, AMV-B, or AMV-C. Approximately 24 h after infection, the yolk sac cultures were overlayed with 3 ml of medium containing 0.7% agar (Difco Laboratories, Detroit, Mich.). The cultures were overlayed every 4 days with 2.5 ml of medium containing 0.7% agar. Foci of leukemic myeloblasts (clones) were picked from the AMV-infected yolk sac cells and cultured on chicken embryonic fibroblast feeder layers irradiated with 10,000 rads until they reached a concentration of approximately 5×10^6 cells/ml.

Two approaches were taken to isolate clones of leukemic myeloblasts which would not contain helper proviral DNA as determined by Southern blot analysis. First, $L7_2$ C/ABE yolk sac cultures were infected with AMV-S which contains subgroup A and B viruses at a high multiplicity of infection (MOI), i.e., leukemic plasma diluted fivefold. Only one $L7_2$ clone, 333E10, out of 50 originally isolated multiplied to more than 5×10^6 cells and was analyzed by blot analysis. The second approach was to use Hubbard cross chickens selected for their unusually fast growth characteristics and hardiness. Hubbard cross yolk sac cultures were infected with AMV-S at a 5-, 50-, or 500-fold dilution of AMV-S. Leukemic myeloblast clones isolated from cells infected at the higher dilutions of AMV-S should be more likely to contain only the AMV genome. Two clones, HL25D2 and HL25C39, out of 35 isolated from cultures infected at the lowest MOI multiplied to more than 10^8 cells.

Isolation and restriction endonuclease digestion of leukemic myeloblast DNA. High-molecular-weight DNA was isolated from leukemic myeloblast clones by the Hirt procedure for clones consisting of more than 10^8 cells and by the procedure described by Gross-Bellard et al. (5) for clones with 10^8 cells or less. Digestion of cellular DNA with restriction endonucleases has been described (15).

The DNAs from the three AMV-B-induced leukemic myeloblast clones were run on sucrose gradients as described by Maniatis et al. (9) to separate high-molecular-weight cellular DNA from linear proviral DNA which had been detected by *Eco*RI analysis. DNA greater than 30 kilobases was selected from the sucrose gradients and ethanol precipitated. This DNA was resuspended in water and used for *Kpn*I analysis.

Isolation of λ proviral DNA recombinant phage. A library of λ chicken recombinant phage was created by inserting 16- to 20-kilobase fragments of *Eco*RI partially digested DNA from leukemic myeloblasts into λ charon 4a (17). The DNA was isolated from AMV-B virus-producing leukemic myeloblasts taken from the peripheral blood of chicken 21710 (16). Two of six recombinants detected by hybridization with AMV-S ^{125}I-labeled RNA were used to prepare high-titer stocks for subsequent DNA purification as described by Souza et al. (17).

Restriction endonuclease cleavage of DNA from λ hybrids. Restriction endonucleases, *Eco*RI, *Hin*dIII, *Xba*I, and *Bam*HI were prepared in our laboratory. *Kpn*I, *Xho*I, and *Bgl*II were purchased from New England Biolabs, Beverly, Mass. Digestions of 0.5 μg of λ proviral recombinant DNAs were carried out with a three- to fivefold excess of the appropriate enzyme under the following conditions: *Eco*RI, 100 mM Tris (pH 7.4), 10 mM $MgCl_2$, and 50 mM NaCl; *Hin*dIII, 10 mM Tris (pH 7.4), 10 mM $MgCl_2$, 60 mM NaCl, and 50 μg of gelatin per ml (Difco); *Xba*I, 6 mM Tris (pH 7.4), 6 mM $MgCl_2$, 6 mM 2-mercaptoethanol (2-ME), 150 mM NaCl, and 50 μg of gelatin per ml; *Bam*HI, 6 mM Tris (pH 7.4), 6 mM $MgCl_2$, 6 mM 2-ME, 50 mM NaCl, and 50 μg of gelatin per ml; *Xho*I, 6 mM Tris (pH 7.4), 6 mM $MgCl_2$, 6 mM 2-ME, 150 mM NaCl, and 50 μg of gelatin per ml; *Bgl*II, 10 mM Tris (pH 7.4), 10 mM $MgCl_2$, 1 mM dithiothreitol, 60 mM KCl, and 50 μg of gelatin per ml; and *Kpn*I, 6 mM Tris (pH 7.4), 6 mM $MgCl_2$, 6 mM 2-ME, 6 mM NaCl, and 50 μg of gelatin per ml.

^{125}I labeling of RNA. AMV-S 35S or 70S RNA was iodinated with ^{125}I (Amersham Corp., Arlington Heights, Ill.) to a specific activity of approximately 2×10^8 cpm/μg as reported by Souza and Baluda (15).

Agarose gels, transfer, hybridization, and autoradiography. Restriction endonuclease-digested cellular DNA was electrophoresed in 0.7% agarose gels (Sigma Chemical Co., St. Louis, Mo.; low electroendosmosis) and further treated as described in the accompanying paper (16). Restriction endonuclease-digested λ hybrid DNA was electrophoresed in 1.2% agarose gels containing ethidium bromide (0.4 μg/ml). Gels were photographed with a Polaroid camera, using Polaroid type 55 film; then the gels were prepared for blotting. The internal proviral *Eco*RI fragments from the two λ proviral recombinants were purified by electrophoretic fractionation of total *Eco*RI digests in a Seaplaque gel (Seakem low-temperature-melting agarose, Marine Colloids, Rockland, Maine). The DNA fragments were eluted from the gel after adding 5 volumes of buffer C (50 mM Tris, pH 8.0, 10 mM EDTA, and 10 mM NaCl) and melting the agarose at

65°C for 10 min. This was followed by two phenol extractions at 37°C, two chloroform extractions at room temperature, and two ether extractions. The DNA was ethanol precipitated and resuspended in water.

Physical and biological containment. This work was carried out at the P2-EK2 containment levels as stated in the revised guidelines of the National Institutes of Health (1978).

RESULTS

Identification and restriction endonuclease mapping of λ chicken recombinants containing AMV or MAV proviral DNA. The λ proviral recombinants could contain either endogenous, AMV, or MAV-1-like proviral DNA, which can be distinguished from one another by analysis of *Eco*RI and *Hin*dIII blots. One recombinant, λ11A1-1, has been partially characterized with the restriction enzymes *Eco*RI and *Hin*dIII (17) and contains the entire putative AMV genome as evidenced by the presence of an *Eco*RI 2.2-Md fragment (Fig. 1b, b′) and *Hin*dIII 2.6- and 1.95-Md fragments (Fig. 1d, d′).

A second recombinant, λ10A2-1, contained MAV-1-like proviral DNA as demonstrated by the presence of an *Eco*RI 2.6-Md fragment and *Hin*dIII 1.95-Md fragment (Fig. 1c,c′ and e,e′). λ10A2-1 did not contain a complete MAV-1-like provirus because *Eco*RI generated only one juncture fragment (5.1 Md) (Fig. 1c′). Since the MAV viral DNAs integrate colinearly with respect to linear viral DNA (3), a second *Eco*RI juncture fragment should have been present. A *Hin*dIII blot of λ10A2-1 revealed fragments of 5.6 and 0.25 Md in addition to the MAV-1-like 5′-proximal 1.95-Md fragment (Fig. 1e′). All the internal fragments generated in an *Eco*RI-*Hin*dIII double digest of MAV-1 linear viral DNA (2.3, 1.6, 0.8, and 0.3 Md) (3), except for the 0.8-Md fragment which represents 3′-proximal viral DNA, were present in λ10A2-1 (Fig. 1g′). This demonstrates that λ10A2-1 lacks MAV-1-like proviral DNA beyond the 3′-proximal *Eco*RI site. The analyses of λ10A2-1 by *Eco*RI, *Hin*dIII, *Eco*RI-*Hin*dIII, and subsequent enzyme digests show that λ10A2-1 contains 85% of a MAV-1-like provirus beginning with 5′ juncture sequences and ending at the 3′-proximal proviral *Eco*RI site, which is adjacent to the right arm of the charon 4a vector.

The MAV-1 *Hin*dIII site near the 3′-proximal *Eco*RI site could not be positioned relative to that *Eco*RI site in linear viral DNA (3). The lack of a *Hin*dIII 2.3-Md fragment in the MAV-1-like proviral DNA of λ10A2-1 now permits us to position this *Hin*dIII site on the 3′ side of the 3′-proximal *Eco*RI site.

There are two *Hin*dIII sites in the linear DNA of ASVs positioned within 0.1 Md of each other approximately 2.1 Md from the 5′ end (13, 18). In our previous studies, only one *Hin*dIII site was apparent at this position in MAV-1 and MAV-2 linear DNAs (3). By isolating the internal *Eco*RI proviral fragments from λ10A2-1 (2.6-Md MAV-1-like) (Fig. 2b) or λ11A1-1 (2.2-Md AMV) (Fig. 2d) and subjecting these fragments to partial digestion with *Hin*dIII, we could determine whether a second *Hin*dIII site exists in these fragments. If only one *Hin*dIII site exists, then three fragments should be generated after partial digestion with *Hin*dIII. If two sites exist, however, six fragments should be generated with two sets of two fragments differing by approximately 0.1 Md in addition to the uncut fragment and a fragment of 0.1 Md which would not be detectable in our gels. *Hin*dIII partial digestion of either the AMV or MAV internal *Eco*RI

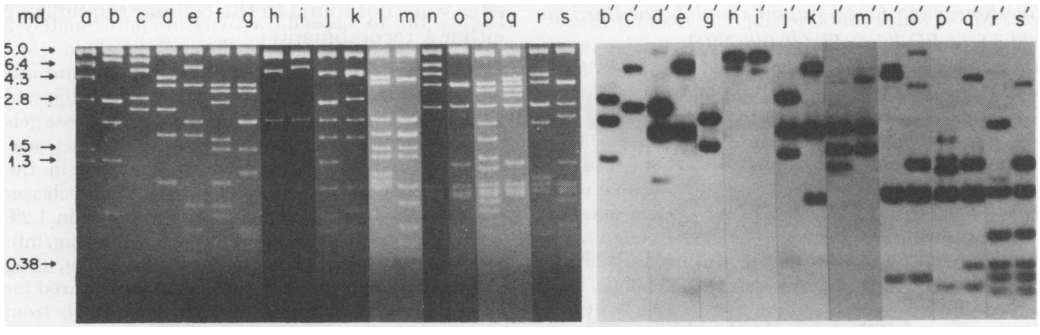

FIG. 1. *Ethidium bromide stains (lanes b–s) and Southern blots (lanes b′–s′) of restriction endonuclease-cleaved λ11A1-1 (presumptive AMV) and λ10A2-1 (MAV-1-like). Ethidium bromide stain of HindIII-cleaved λ⁺ DNA is shown in lane a. EcoRI: (b, b′) 11A1-1, (c, c′) 10A2-1. HindIII: (d, d′) 11A1-1, (e, e′) 10A2-1. EcoRI-HindIII: (f) 11A1-1, (g, g′) 10A2-1. KpnI: (h, h′) 11A1-1, (i, i′) 10A2-1. KpnI-EcoRI: (j, j′) 11A1-1, (k, k′) 10A2-1. KpnI-HindIII: (l, l′) 11A1-1, (m, m′) 10A2-1. BamHI: (n, n′) 11A1-1, (o, o′) 10A2-1. BamHI-EcoRI: (p, p′) 11A1-1, (q, q′) 10A2-1. BamHI-HindIII: (i, i′) 11A1-1, (s, s′) 10A2-1.*

fragment yielded the patterns expected for two *Hin*dIII sites separated by 0.1 Md (Fig. 2c, e). The small set of doublets (at 0.35 Md) common to both AMV and MAV are not readily detectable in Fig. 2c and e, but were seen in a longer exposure. Thus, these two *Hin*dIII sites appear to be conserved in the AMV-S viral DNAs, as well as in the ASV viral DNAs.

The *Eco*RI and *Hin*dIII sites in the chicken proviral DNA inserts of λ11A1-1 and λ10A2-1 were mapped by a combination of ethidium bromide staining (Fig. 1b–g) and Southern blotting (Fig. 1b′–e′, g′). In λ10A2-1, only the *Hin*dIII site adjacent the proviral DNA in the cellular sequences could be mapped, but at least three other *Hin*dIII sites exist in the cellular sequences. *Hin*dIII digestion of the two λ recombinants showed that both the putative AMV and MAV-like proviruses had integrated colinearly with respect to their linear viral DNA.

Using five additional enzymes with hexanucleotide recognition sites, we derived the physical maps of λ10A2-1 and λ11A1-1 presented in Fig. 3. Ethidium bromide stains and autoradiographs of Southern blots of *Kpn*I, *Kpn*I-*Eco*RI, and *Kpn*I-*Hin*dIII digests of λ11A1-1 and λ10A2-1 are shown in Fig. 1h–m and h′–m′. The proviral sequences in each λ recombinant contained one *Kpn*I site (Fig. 3), but no *Kpn*I sites existed in the cellular sequences. Similar sets of single and double digests were also done and analyzed for *Bam*HI (Fig. 1n–s and 1n′–s′) and *Bgl*II (Fig. 4b–g and 4b′–g′) sites. The proviral sequences in the presumptive AMV clone contained four *Bam*HI sites and two *Bgl*II sites, whereas the MAV-1-like proviral sequences contained five *Bam*HI sites and two *Bgl*II sites (Fig. 3). The cellular sequences adjacent to the 3′ end of the presumptive AMV provirus contained one *Bam*HI site, but no other *Bam*HI sites were present in the cellular sequences of either λ recombinant. *Bgl*II sites were not mapped in the cellular sequences of either recombinant. *Xho*I and *Xba*I sites were mapped by single digests (Fig. 4h, i, h′, i′ and 4l, m, l′, m′) and by double digests with *Kpn*I (Fig. 4j, k, j′, k′ and 4n, o, n′, o′). The putative AMV proviral sequences contained two *Xho*I and two *Xba*I sites, whereas the MAV-1-like proviral sequences contained two *Xho*I sites but only one *Xba*I site (Fig. 3). The cellular sequences adjacent to the 3′ end of the presumptive AMV provirus contained one *Xba*I site, as did the cellular sequences adjacent to the 5′ end of the MAV-1-like provirus (Fig. 3). *Xho*I sites were not found in the cellular sequences of either λ recombinant.

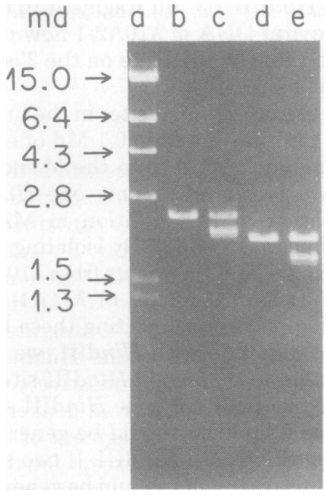

FIG. 2. *Ethidium bromide stains of (a) HindIII-digested λ⁺, (b) MAV-1-like proviral EcoRI 2.6-Md fragment, (c) MAV-1-like proviral EcoRI 2.6-Md fragment partially digested with HindIII, (d) presumptive AMV proviral EcoRI 2.2-Md fragment, and (e) presumptive AMV proviral EcoRI 2.2-Md fragment partially digested with HindIII. Both HindIII partial digestions were done for approximately one-third the time necessary for complete digestion.*

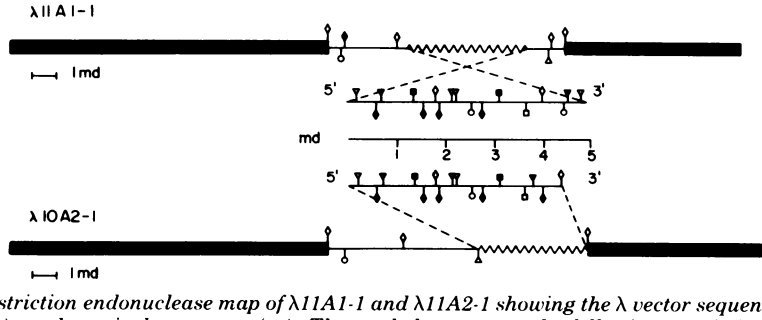

FIG. 3. *Restriction endonuclease map of λ11A1-1 and λ11A2-1 showing the λ vector sequences (▬), cellular sequences (—), and proviral sequences (〰). The symbols represent the following restriction endonucleases: (▽) HindIII, (◆) BamHI, (▼) XhoI, (■) BglII, (◇) EcoRI, (○) XbaI, and (□) KpnI. The enlargements represent the proviral DNA at twice the scale of the whole recombinant. The presumptive AMV proviral DNA is inverted for comparing enzyme sites 5′ to 3′.*

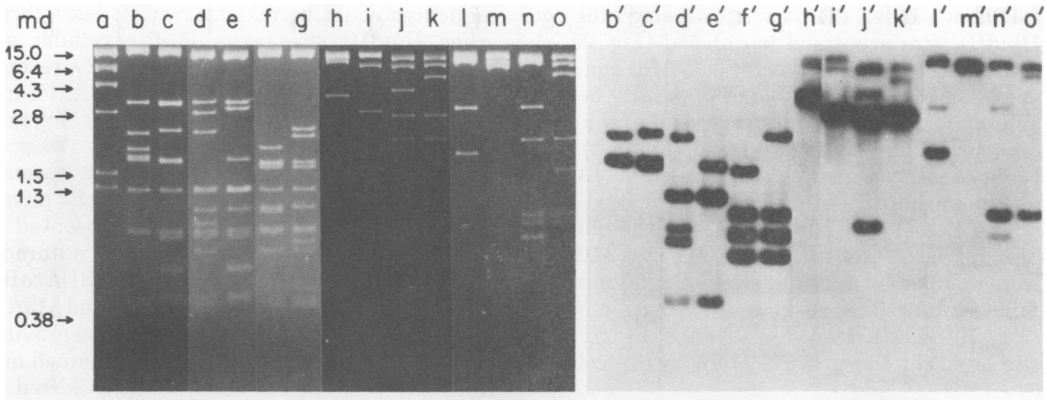

FIG. 4. *Ethidium bromide stains (b–o) and Southern blots (b'–o') of restriction endonuclease-cleaved λ11A1-1 (presumptive AMV) and λ10A2-1 (MAV-1-like). Ethidium bromide stain of HindIII-cleaved λ⁺ DNA is shown in lane a. BglII: (b, b') 11A1-1, (c, c') 10A2-1. BglII-EcoRI: (d, d') 11A1-1, (e, e') 10A2-1. BglII-HindIII: (f, f') 11A1-1, (g, g') 10A2-1. XhoI: (h, h') 11A1-1, (i, i') 10A2-1. XhoI-KpnI: (j, j') 11A1-1, (k, k') 10A2-1. XbaI: (l, l') 11A1-1, (m, m') 10A2-1. XbaI-KpnI: (n, n') 11A1-1, (o, o') 10A2-1.*

The polarity of the proviral DNA in λ11A1-1 (with respect to viral RNA) was opposite the polarity of the proviral DNA in λ10A2-1 (Fig. 3). All the enzyme sites in the proviral sequences of the putative AMV or partial MAV-1-like genomes mapped identically from the 5'-proximal *Hin*dIII site and up to the *Kpn*I site. Between the *Kpn*I site and the 3'-proximal *Eco*RI site in the MAV-1-like proviral DNA there were two enzyme sites (one *Xho*I and one *Bam*HI) which were not present in the same region of the putative AMV provirus. The difference in mass (0.4 Md) between the two *Kpn*I-*Eco*RI fragments from the MAV-1-like and the putative AMV proviruses corresponds to the total difference in mass between the two proviruses (3, 17). The enzyme sites on the 3' side of the 3'-proximal *Eco*RI site in the putative AMV and MAV-1-like proviruses could not be compared because that portion of the provirus is not present in the partial MAV-1-like λ recombinant. The variation in number and position of enzyme sites in the cellular sequences adjacent to the proviral DNA in each λ recombinant shows that each provirus had integrated at a different location in the chicken genome.

***Hin*dIII analysis of DNA from leukemic myeloblast clones induced by AMV-S or AMV-B.** DNAs from three Spafas C/E AMV-B-induced leukemic myeloblast clones (13-3A1, 13-3A5, and 13-3C9), one $L7_2$ C/ABE AMV-S-induced leukemic myeloblast clone (333E10), and five Hubbard cross AMV-S-induced leukemic myeloblast clones (HL25D2, HL2500A3, HL250C11, HL2500B61, and HL25C39) were analyzed with *Hin*dIII (Fig. 5). *Hin*dIII-digested DNA from Spafas C/E embryo 13-3 (Fig. 5a), Hubbard embryo HL2 (Fig. 5f), and $L7_2$ embryo 333 (Fig. 8a) served as controls to show the endogenous proviral DNA background. All the leukemic myeloblast clones contained a *Hin*dIII 2.6-Md DNA fragment (Fig. 5), indicating the presence of the putative AMV genome (17). All the clones also contained a *Hin*dIII 1.95-Md fragment. This fragment comigrated with an endogenous fragment in the Hubbard chicken DNA but was clearly quantitatively different in intensity in the DNA from leukemic myeloblasts. A third *Hin*dIII fragment of 0.8 Md was present in all the clones except for the AMV-S-induced $L7_2$ C/ABE 333E10 clone and an AMV-S induced Hubbard clone (HL25D2 low MOI). The 0.8-Md fragment indicates the presence of MAV-1 (3) or the MAV-1-like genome present in AMV-B virus preparations (16). Therefore, of the nine AMV-B and AMV-S clones examined, seven contained both the putative AMV genome and a MAV-1-like helper and two contained only the putative AMV genome.

Supernatant from clone 333E10 did not induce formation of leukemic myeloblasts in C/E yolk sac cultures, whereas the supernatant from three other clones tested, AMV-B-induced clone 13-3A5 and AMV-C-induced clones 333B4 and 333C1, converted C/E yolk sac cultures. Therefore, in clone 333E10 the absence of helper proviral DNA is correlated with the inability to produce leukemogenic virus (AMV), whereas three of the clones containing helper provirus were able to produce AMV.

A faint *Hin*dIII fragment of approximately 3.1 Md could be detected in AMV-B clone 13-3C9 (Fig. 5d). This fragment was similar in size to that expected for MAV-2 (3.1 Md) and probably was not a juncture fragment, since other juncture fragments could not be detected in any of

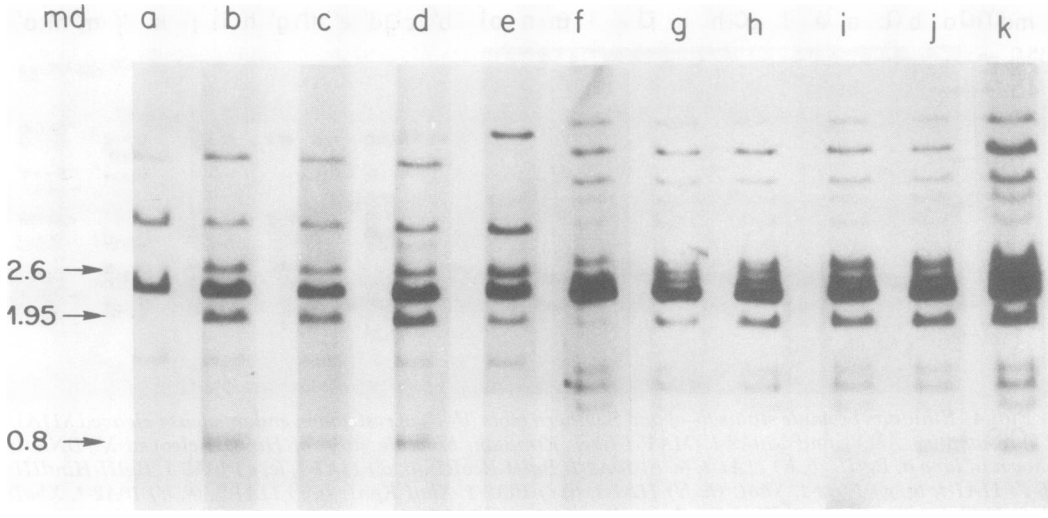

FIG. 5. *HindIII blots of AMV-B (b–d) and AMV-S (e, g–k) leukemic myeloblast clone DNAs. (a) Spafas C/E 13-3 embryo, (b) 13-3A1, (c) 13-3A5, (d) 13-3C9, (e) 333E10, (f) Hubbard HL2 embryo, (g) HL25D2, (h) HL2500A3, (i) HL250C11, (j) HL2500B61, and (k) HL25C39.*

the clones whose DNA was treated with *Hin*dIII. This fragment may be the result of a recombination event between different viral DNAs.

All of the *Hin*dIII-treated DNAs from AMV-B- and AMV-S-induced leukemic myeloblast clones generated fragments identical in mass to those generated by *Hin*dIII cleavage of MAV-1 and putative AMV linear viral DNA (3). This demonstrates that both the putative AMV provirus and the MAV-1-like provirus integrate colinearly with respect to linear viral DNA.

***Eco* RI and *Kpn*I analyses of DNA from leukemic myeloblast clones induced by AMV-S or AMV-B.** The restriction enzyme map of the putative AMV provirus presented in Fig. 3 indicates that *Eco*RI and *Kpn*I would be appropriate enzymes for the detection of AMV juncture fragments. Comparison of the MAV-1 linear viral DNA restriction map (3) with that presented in Fig. 3 also indicates that *Kpn*I and *Eco*RI are suitable for detection of MAV-1 juncture fragments. Both enzymes should generate two juncture fragments containing sufficient proviral DNA for detection. We have been unable to find an enzyme which does not cleave the viral DNAs of the AMV-S virus complex.

*Eco*RI blots of DNA from leukemic myeloblast clones induced by AMV-S or AMV-B revealed zero, one, or two juncture fragments (Fig. 6). Because of the small number (2×10^7 to 8×10^7 cells) of myeloblasts in each AMV-B-induced clone, the Hirt procedure was not used for DNA isolation. Consequently, some linear viral DNA intermediates were present as demonstrated by the generation of *Eco*RI fragments of 4.4, 1.8, and 0.9 Md. All the leukemic myeloblast clones contained an *Eco*RI 2.2-Md fragment characteristic of the putative AMV genome. In clone 333E10 (Fig. 6e), this fragment comigrated with an endogenous fragment but it was clearly quantitatively different from the endogenous fragment detectable in the embryonic DNA (Fig. 9a). Some of the juncture fragments in the *Eco*RI digests of DNA from the different AMV-B-induced clones appeared to have the same molecular mass (Fig. 6b–d). However, the use of a second enzyme, *Kpn*I, showed that in those myeloblast clones which had *Eco*RI juncture fragments of similar size, the exogenous proviruses were actually integrated at different sites (Fig. 7b–d). *Kpn*I digestion revealed from one to six juncture fragments in DNA from the various AMV-S- and AMV-B-induced leukemic myeloblast clones (Fig. 7).

All of the AMV-B and AMV-S clones revealed at least one juncture fragment if analyzed with both *Eco*RI and *Kpn*I. Some clones contained zero or an odd number of juncture fragments after either an *Eco*RI or *Kpn*I digestion. This was probably due to the comigration of some juncture fragments with endogenous fragments or with internal fragments of the exogenous proviruses. Another possibility could be that incomplete proviruses lacking some *Eco*RI or *Kpn*I sites might have been integrated. In this case, fewer juncture fragments could be generated after digestion with these two enzymes. However, this alternative does not appear likely because all the leukemic myeloblast clones contained all the *Hin*dIII internal fragments of the

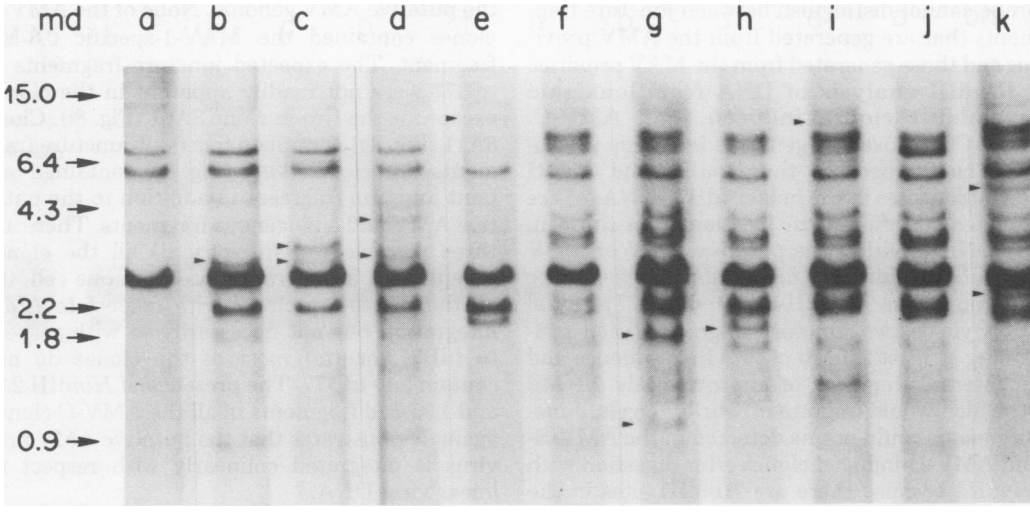

FIG. 6. *EcoRI blots of AMV-B (b–d) and AMV-S (e, g–k) leukemic myeloblast clone DNAs. (a) Spafas C/E 13-3 embryo, (b) 13-3A1, (c) 13-3A5, (d) 13-3C9, (e) 333E10, (f) Hubbard HL2 embryo, (g) HL25D2, (h) HL2500A3, (i) HL250C11, (j) HL2500B61, and (k) HL25C39. The arrowheads point to the juncture fragments detected in the individual clones.*

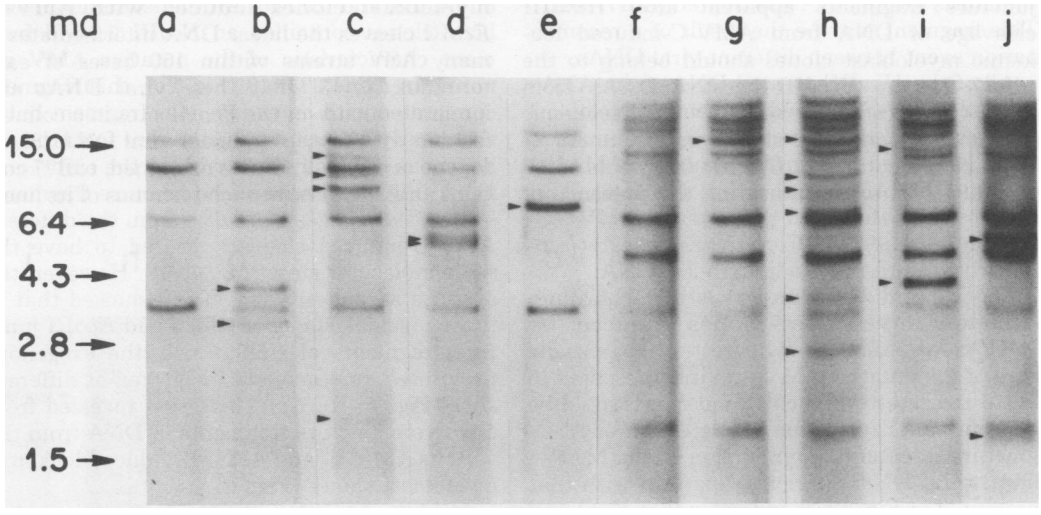

FIG. 7. *KpnI blots of AMV-B (b–d) and AMV-S (e, g–j) leukemic myeloblast clone DNAs. (a) Spafas C/E 13-3 embryo, (b) 13-3A1, (c) 13-3A5, (d) 13-3C9, (e) 333E10, (f) Hubbard HL2 embryo, (g) HL25D2, (h) HL250C11, (i) HL2500B61, and (j) HL25C39. The arrowheads point to the juncture fragments detected in the individual clones. DNA 30 kilobases or larger from the AMV-B clones was selected from sucrose gradients for KpnI digestion.*

appropriate genomes present. The *Hin*dIII analysis combined with the enumeration of *Eco*RI or *Kpn*I juncture fragments indicated that the individual myeloblast clones contained from one to three proviruses per cell, each integrated at a different site. Even the two Hubbard clones (HL2500A3 and HL2500B61) isolated from cultures infected at high MOI (100 or more infectious units/cell) appeared to contain only two exogenous proviruses per cell. Juncture fragment analysis was also consistent with the presence of only one exogenously introduced provirus (AMV) in clones 333E10 and HL25D2 as suggested by the *Hin*dIII analysis.

The putative AMV genome shares extensive sequence homology with the helper MAV-1-like genome as evidenced by the restriction maps of the two genomes. Therefore, our hybridization

probe cannot distinguish between juncture fragments that are generated from the AMV provirus and those generated from the MAV provirus.

***Hind*III analysis of DNA from leukemic myeloblast clones induced with AMV-C.** AMV-C was used to generate leukemic myeloblast clones because the *Hind*III and *Eco*RI restriction sites in the helper tdB77 DNA (4) are sufficiently different in location from those in the DNA of either the putative AMV or MAV genomes to allow easy distinction between those proviral DNAs. *Hind*III-digested tdB77 proviral DNA yields two juncture fragments each containing at least 2.0 Md of proviral sequence and an internal fragment of approximately 0.1 Md (4) which would migrate off our 0.7% gels. Juncture bands could not be detected in the AMV-S- and AMV-B-induced clones after digestion with *Hind*III because there are *Hind*III sites in the proviral DNAs of the putative AMV or MAV genomes very close to the cell-provirus junctions. This does not leave sufficient viral DNA in the *Hind*III juncture fragments to be detected with our experimental approach. Therefore, any juncture fragments apparent after *Hind*III cleavage of DNA from AMV-C-induced leukemic myeloblast clones should belong to the tdB77 helper. *Hind*III-digested DNAs from AMV-C-induced $L7_2$ and H&N C/O leukemic myeloblast clones are shown in Fig. 8. All of these clones contained *Hind*III fragments of 2.6 and 1.95 Md, again indicating the presence of the putative AMV genome. None of the AMV-C clones contained the MAV-1-specific 0.8-Md fragment. The expected juncture fragments of tdB77 were not readily apparent in the clones except for the two in clone 8A61 (Fig. 8i). Clone 8A11 (Fig. 8g) contained five faint juncture fragments, and clone 333A1 (Fig. 8c) contained one faint juncture fragment in addition to the putative AMV and endogenous fragments. There are three possible explanations: (i) all the clones except 8A61 arose from more than one cell, (ii) all the clones are clonal with respect to AMV integration but not necessarily so with respect to tdB77, or (iii) most of the clones do not contain any tdB77. The presence of *Hind*III 2.6- and 1.95-Md fragments in all the AMV-C clones again demonstrates that the putative AMV provirus is integrated colinearly with respect to linear viral DNA.

AMV-C clone 333B2 (Fig. 8d) also contained a *Hind*III fragment of approximately 3.1 Md as did AMV-B clone 13-3C9 (Fig. 5d), for which we have no solid explanation.

***Eco*RI and *Kpn*I analysis of leukemic myeloblast clones induced with AMV-C.** *Eco*RI cleaves the linear DNA intermediates of many ASV strains within 150 bases of each terminus (6, 13, 18). These viral DNAs also integrate outside of the *Eco*RI sites in a colinear fashion with respect to linear viral DNA (8). As for the other ASV viruses examined, tdB77 contains an *Eco*RI site at each terminus of its linear

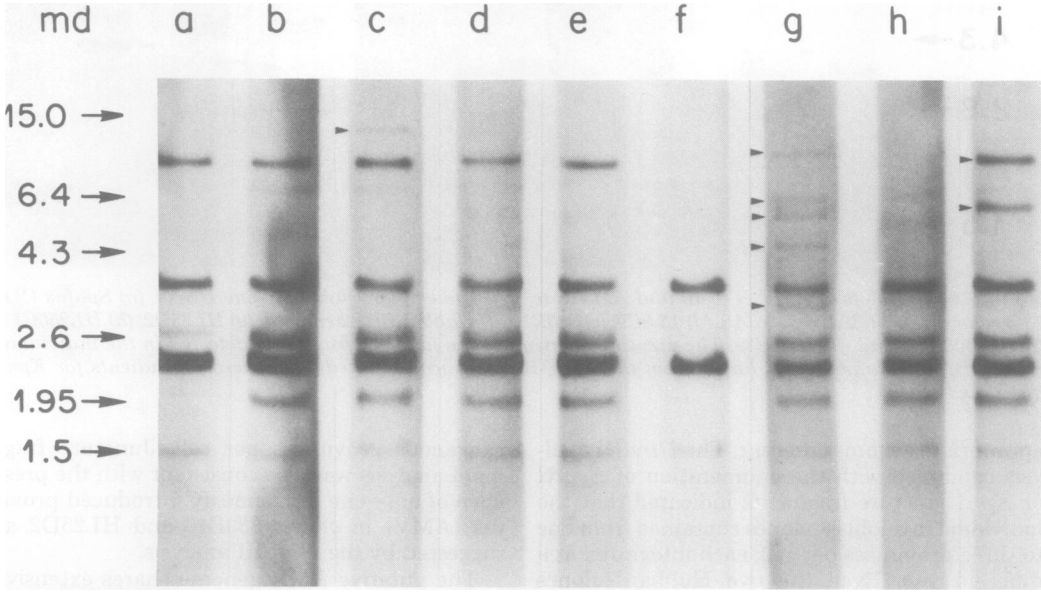

FIG. 8. *HindIII blots of AMV-C leukemic myeloblast clone DNAs. (a) $L7_2$ C/ABE 333 embryo, (b) 333B4, (c) 333A1, (d) 333B2, (e) 333C1, (f) H&N C/O 8 embryo, (g) 8A11, (h) 8A3, and (i) 8A61. The arrowheads point to tdB77 juncture fragments detected in the individual clones.*

viral DNA and at two other internal sites (4). Thus, for the same reason we cannot detect *Hin*dIII juncture fragments in integrated putative AMV or MAV genomes from cloned cells, we would not expect to detect the *Eco*RI juncture fragments of tdB77. However, we should be able to detect the *Eco*RI 1.7- and 0.9-Md internal fragments of tdB77 if its genome is present. The 2.6-Md fragment would comigrate with an endogenous fragment of the same mass. Any additional fragments observed in *Eco*RI digests should then represent juncture fragments of the putative AMV provirus. All the clones contained the AMV-specific *Eco*RI 2.2-Md fragment, although it could only be seen as a quantitative difference in the $L7_2$ C/ABE clones (Fig. 9). The *Eco*RI 2.2-Md fragment was clearly seen in the H&N C/O clones (Fig. 9g–i) which were derived by infecting H&N C/O yolk sac cells with AMV-C supernatant from the leukemic myeloblasts of clone 333B4. All of the clones contained tdB77 proviral DNA as evidenced by the appearance of the 1.7- and 0.9-Md fragments (Fig. 9). The presence of these two fragments in all of the AMV-C clones demonstrated that tdB77 also integrates colinearly with respect to its linear viral DNA (4). From one to three *Eco*RI juncture bands were detected in the AMV-C clones (Fig. 9). Clones 333B2 and 333Cl showed three *Eco*RI juncture bands each, but only two should have been detected if one AMV provirus was present. A third fragment indicates that these two clones could have originated from two converted cells. Two of the three probable juncture fragments (4.4 and 1.8 Md) in clone 333B2 (Fig. 9d) could represent the presence of free linear viral DNA; however, *Kpn*I digestion did not support this possibility. The expected *Kpn*I linear DNA fragments (3.6 and 1.7 Md for tdB77 or 3.6 and 1.3 Md for AMV) were not present.

*Kpn*I cleaves the putative AMV genome once and should also cleave tdB77 once because B77 contains one *Kpn*I site (13, 18), and the restriction map for five other enzymes used on tdB77 is identical to that for B77 (except for sites in the *src* gene) (4). From one to five juncture bands were apparent after *Kpn*I digestion of DNA from the AMV-C-induced leukemic myeloblast clones (Fig. 10).

Restriction endonuclease analyses of the AMV-C clones indicated that they all contained the tdB77 and the putative AMV genomes. *Eco*RI analysis showed that the presumptive AMV genome can integrate at many different sites in the cellular DNA.

DISCUSSION

Restriction endonuclease analyses of two λ chicken recombinants have shown that λ11A1-1 contains the putative AMV provirus flanked on either side by cellular sequences and that λ10A2-

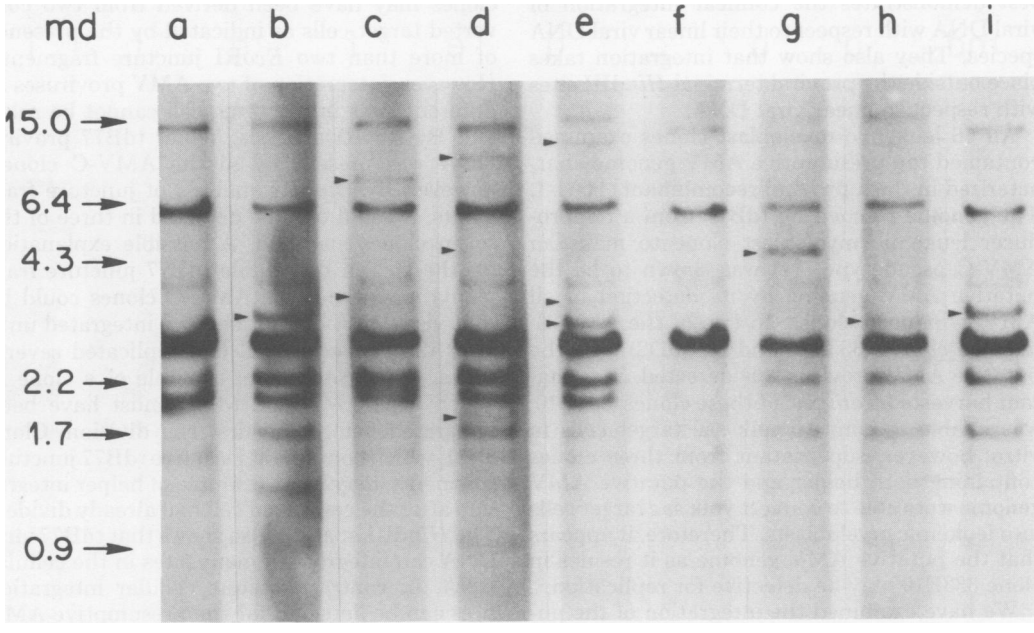

FIG. 9. *EcoRI blots of AMV-C leukemic myeloblast clone DNAs. (a) $L7_2$ C/ABE 333 embryo, (b) 333B4, (c) 333A1, (d) 333B2, (e) 333C1, (f) H&N C/O 8 embryo, (g) 8A11, (h) 8A3, and (i) 8A61. The arrowheads point to AMV juncture fragments in the individual clones.*

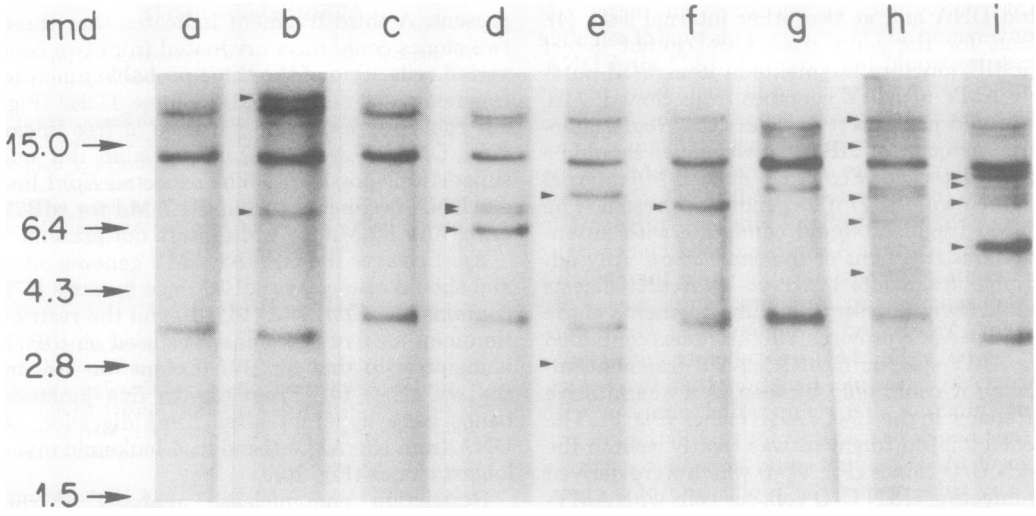

FIG. 10. *KpnI blots of AMV-C leukemic myeloblast clone DNAs. (a) L7₂ C/ABE 333 embryo, (b) 333B4, (c) L7₂ C/ABE 333 embryo, (d) 333A1, (e) 333B2, (f) 333C1, (g) H&N C/O 8 embryo, (h) 8A11, and (i) 8A61. The arrowheads point to the juncture fragments in the individual clones. The gels for blots a, b, and i were run slightly longer than the gels for the other blots.*

1 contains 85% of a MAV-1-like provirus with cellular sequences adjacent to the 5′ end of the provirus. Restriction enzyme mapping of the cellular sequences present in the two λ proviral recombinants clearly indicates a difference in the cellular location of the two integrated proviruses. *Hin*dIII analysis of these λ recombinants best demonstrates the colinear integration of viral DNA with respect to their linear viral DNA species. They also show that integration takes place outside the proviral terminal *Hin*dIII sites with respect to linear viral DNA.

All 16 leukemic myeloblast clones examined contained the presumptive AMV genome characterized in the λ proviral recombinant, 11A1-1. The genome rescued by tdB77 from a nonproducer leukemic myeloblast clone to make an AMV-C pseudotype (11) was shown to be the putative AMV genome by its detection in all AMV-C-induced clones. In two of the AMV-S-induced clones (333E10 and HL25D2) only the putative AMV provirus was detected. Supernatant harvested from one of these clones, 333E10, was unable to convert yolk sac target cells in vitro; however, supernatant from three clones containing both helper and the putative AMV genome were able to convert yolk sac target cells into leukemic myeloblasts. Therefore, it appears that the putative AMV genome as it resides in clone 333E10 may be defective for replication.

We have examined the integration of the putative AMV provirus and the various helper proviruses in leukemic myeloblast clones by comparing juncture fragments generated by restriction endonuclease digestion. *Eco*RI juncture fragments of various sizes belonging to the putative AMV provirus were detected in all the AMV-C-induced clones, demonstrating that multiple cellular sites are suitable for integration of this provirus. Two of the AMV-C-induced clones may have been derived from two converted target cells as indicated by the presence of more than two *Eco*RI juncture fragments. However, integration of two AMV proviruses at different sites in the same cell cannot be ruled out. By *Eco*RI analysis, helper tdB77 proviral DNA was present in all the AMV-C clones; however, by *Hin*dIII analysis of juncture fragments, it could only be detected in three of the seven clones analyzed. A possible explanation for the lack of detectable tdB77 juncture fragments in some of the AMV-C clones could be that viral DNA did not become integrated until after the converted cell had replicated several times. Clone 8A61 is an example of a clone in which both AMV and tdB77 must have been integrated before the first cell division. Clone 8A11, which contains at least five tdB77 juncture fragments, may be an example of helper integration after the converted cell had already divided. The *Hin*dIII analysis also shows that tdB77 viral DNA can integrate at many sites in the cellular DNA. In contrast, unique cellular integration sites can be detected for the presumptive AMV provirus in all the AMV-C-induced clones, suggesting that integration of the presumptive

AMV DNA may be necessary for target cell conversion and replication. This type of selective pressure would not exist for tdB77 viral DNA. These findings provide additional evidence that the presumptive AMV genome is the agent responsible for acute myeloblastic leukemia. Since juncture fragments of the putative AMV provirus can be detected in all AMV-C-induced clones, then most of the juncture fragments in the AMV-B- and AMV-S-induced clones must represent additional sites in which the putative AMV genome can integrate. Only two of the seven AMV-B and AMV-S clones which contained both the MAV-1-like helper and the putative AMV genomes had more than two detectable juncture fragments after analysis with either *Eco*RI or *Kpn*I. As for tdB77, the integration of MAV helpers could also have occurred at any time during the replication of a clone. The analyses of the two clones (13-3A5 and HL250C11) which contain four or more *Kpn*I juncture fragments and of the MAV-1-like λ chicken recombinant suggest that the integration of MAV-1-like helper provirus can take place at a minimum of three or four sites and probably at as many sites as AMV does. The use of more sensitive techniques has led to the current understanding of the great variation in quantity and arrangement of endogenous proviruses. Consequently, the previous model based on a simpler endogenous provirus arrangement that lead to the interpretation that AMV might integrate in tandem with the endogenous provirus is no longer adequate (14). The *Hin*dIII analysis showed that the presumptive AMV or helper viral DNA integrates colinearly with respect to linear viral DNA in all the leukemic myeloblast clones.

The putative AMV provirus has a mass of approximately 4.9 Md (17) or about 0.4 Md smaller than the MAV proviruses (5.3 Md) (3). By restriction endonuclease analysis, the proviruses of the MAV-1-like and putative AMV genomes are identical from their 5′ terminus extending 3.6 Md to the *Kpn*I site in each genome. This has been confirmed by heteroduplex analysis (L. M. Souza, J. N. Strommer, R. L. Hillyard, M. C. Komaromy, and M. A. Baluda, Proc. Natl. Acad. Sci. U.S.A., in press). The fragment located between the *Kpn*I site and the 3′-proximal *Eco*RI site is approximately 0.4 Md shorter in the presumptive AMV genome than it is in the MAV-1-like genome. The difference in mass between these two fragments corresponds to the total difference in mass between the presumptive AMV and MAV genomes. We have shown that this difference in mass is the result of a substitution for all or most of the *env* gene by a cellular sequence (Souza et al., in press).

ACKNOWLEDGMENTS

We thank J. W. Beard and C. Moscovici for providing viruses and L. B. Crittenden and V. Ryckebosch for providing fertile eggs.

Research was supported by Public Health Service research grant CA-10197 from the National Cancer Institute. L.M.S. Souza was supported by predoctoral institutional national research service award CA-09056 from the National Cancer Institute, Public Health Service. L.M.S. was also a recipient of a predoctoral trainee award from the American Cancer Society, institutional grant IN-131.

LITERATURE CITED

1. **Astrin, S. M.** 1978. Endogenous viral genes of the White Leghorn chicken: common site of residence and sites associated with specific phenotypes of viral gene expression. Proc. Natl. Acad. Sci. U.S.A. **75**:5941–5945.
2. **Baluda, M. A., and I. E. Goetz.** 1961. Morphological conversion of cell cultures by avian myeloblastosis virus. Virology **15**:185–199.
3. **Bergmann, D. G., L. M. Souza, and M. A. Baluda.** 1980. Characterization of avian myeloblastosis-associated virus DNA intermediates. J. Virol. **34**:366–372.
4. **Gilmer, T. M., and J. T. Parsons.** 1979. Analysis of cellular integration sites in avian sarcoma virus-infected duck embryo cells. J. Virol. **32**:762–769.
5. **Gross-Bellard, M., P. Oudet, and P. Chambon.** 1973. Isolation of high-molecular-weight DNA from mammalian cells. Eur. J. Biochem. **36**:32–38.
6. **Hsu, T. W., J. L. Sabran, G. E. Mark, R. V. Guntaka, and J. M. Taylor.** 1978. Analysis of unintegrated avian RNA tumor virus double-stranded DNA intermediates. J. Virol. **28**:810–818.
7. **Hughes, S. H., F. Payvar, D. Spector, R. T. Schimke, H. L. Robinson, G. S. Payne, J. M. Bishop, and H. E. Varmus.** 1979. Heterogeneity of genetic loci in chickens: analysis of endogenous viral and nonviral genes by cleavage of DNA with restriction endonucleases. Cell **18**:347–359.
8. **Hughes, S. H., P. R. Shank, D. H. Spector, H. J. Kung, J. M. Bishop, H. E. Varmus, P. K. Vogt, and M. L. Breitman.** 1978. Proviruses of avian sarcoma virus are terminally redundant, co-extensive with unintegrated linear DNA and integrated at many sites. Cell **15**:1397–1410.
9. **Maniatis, T., R. C. Hardison, E. Lacy, J. Lauer, C. O'Connell, D. Quon, G. K. Sim, and A. Efstratiadis.** 1978. The isolation of structural genes from libraries of eucaryotic DNA. Cell **15**:687–701.
10. **McClements, W., H. Hanafusa, S. Tilghman, and A. Shalka.** 1979. Structural studies on oncornavirus-related sequences in chicken genomia DNA: two-step analyses of Eco RI and Bgl I restriction digests and tentative mapping of a ubiquitous endogenous provirus. Proc. Natl. Acad. Sci. U.S.A. **76**:2165–2169.
11. **Moscovici, C., and M. Zanetti.** 1970. Studies on single foci of hematopoietic cells transformed by avian myeloblastosis virus. Virology **42**:61–67.
12. **Sabran, J. L., T. W. Hsu, C. Yeater, A. Kaji, W. S. Mason, and J. M. Taylor.** 1979. Analysis of integrated avian RNA tumor virus DNA in transformed chicken, duck, and quail fibroblasts. J. Virol. **29**:170–178.
13. **Shank, P. R., S. H. Hughes, H. J. Kung, J. E. Majors, W. Quintrell, R. V. Guntaka, J. M. Bishop, and H. E. Varmus.** 1978. Mapping unintegrated avian sarcoma virus DNA: termini of linear DNA bear 300 nucleotides present once or twice in two species of circular DNA. Cell **15**:1383–1395.
14. **Shoyab, M., M. N. Dastoor, and M. A. Baluda.** 1976. Evidence of tandem integration of avian myeloblastosis virus DNA with endogenous provirus in leukemic

chicken cells. Proc. Natl. Acad. Sci. U.S.A. **73**:1749–1753.

15. **Souza, L. M., and M. A. Baluda.** 1978. Qualitative studies of the endogenous provirus in the chicken genome, p. 217–229. *In* J. Stevens, G. J. Todaro, C. F. Fox (ed.), Persistent viruses. Academic Press, Inc., New York.
16. **Souza, L. M., and M. A. Baluda.** 1980. Identification of the avian myeloblastosis virus genome. I. Identification of restriction endonuclease fragments associated with acute myeloblastic leukemia. J. Virol. **36**:317–324.
17. **Souza, L. M., M. C. Komaromy, and M. A. Baluda.** 1980. Identification of a proviral genome associated with avian myeloblastic leukemia. Proc. Natl. Acad. Sci. U.S.A. **77**:3004–3008.
18. **Taylor, J. M., T. W. Hsu, and M. M. C. Lai.** 1978. Restriction enzyme sites on the avian RNA tumor virus genome. J. Virol. **26**:479–484.